Numerical and Experimental Study for Orifice Plate Using Water and Nano-fluids

R. Afify
Mechanical Engineering Department
Arab Academy for Science, Technology and Maritime Transport
Alexandria, Egypt
rola@aast.edu

A. Fawaz
Egyptian Projects Operation & Maintenance (EPROM)
Alexandria, Egypt
a.fawaz58@student.aast.edu

M. Ata
Mechanical Engineering Department
Arab Academy for Science, Technology and Maritime Transport
Alexandria, Egypt
Mina.saad@aast.edu

K. Ibrahim
Mechanical Engineering Department, Faculty of Engineering, Menofia University, Menofia, Egypt.
kamalabd49@gmail.com

***Abstract*— Industrial technologies aim to save energy and minimize operational costs in pumping systems. Nanofluids, containing nanoparticles suspended in base fluids, are proposed as a solution to improve heat transfer efficiency. However, nanofluid particles have higher viscosity and density, which affects the pressure drop and pumping power, which is crucial for piping system design. In the present study, pressure drops of water and nanofluid Al_2O_3-H_2O across orifice are experimentally and numerically studied. A 2” pipe is used in which an orifice plate was installed. Four orifices are used with 1”, ¾”, ½”, and ¼” inner diameters. Pressure drop results of water show slightly lower values than nanofluids results. However, it is suggested to utilize a higher power pump when working with nanofluid.**

Keywords*— *Nanofluid; Pressure drop; Pumping Power; numerical; Experimental; Orifice.

I. Introduction

Head loss in fluid flow through pipes consists of friction and eddy losses, which arise from sudden changes in pipe geometry like bends [1]. Introducing nanofluids, which are composed of a base fluid and a suspended nanoparticle, which enhance thermal conductivity and efficiency in heating and cooling systems [2- 4]. There are many applications, with research exploring factors affecting nanofluid performance, challenges, and future opportunities [5].

Heat transfer rate is improved depending on the type, size, concentration, and mixing ratios of nanoparticles [6-7]. Do et al. [8] demonstrated that using 3.0 vol% Al_2O_3-H_2O nanofluid in mesh wicked heat pipes made thermal resistance less by 40% with respect to water. Nanofluids are prepared via physical mixing or chemical reduction in order to improve base fluid properties, which affect the specific heat capacity, and thermal conductivity [9].

An experimental study [10] on Al_2O_3-H_2O nanofluid revealed a 35–40% thermal conductivity enhancement and an 80–95% viscosity increase at 30 wt.% Al_2O_3-H_2O, emphasizing the need for optimal nanofluid composition and parameters. During an experiment on a single-tube heat exchanger, Shahrul et al. [11] achieved a better performance of the heat exchanger by using metal oxide nanofluids. Routbort et al. [12] proved that nanofluids have a significant effect on heat transfer rate. Due to the increased viscosity, it may require more pumping power.

Babar and Ali [13] indicated that hyper nanofluids improve heat transfer, but studies on their effects on pipes and fittings are limited, highlighting the need for further research.

II. Numerical Analysis

The present study examines pressure drop in a pipe using water and nanofluid separately. Fig. 1 illustrates a 2D pipeline with a 3mm width orifice, varying in diameter ratio. Flow velocity and pressure will be examined using different inner diameters orifices.

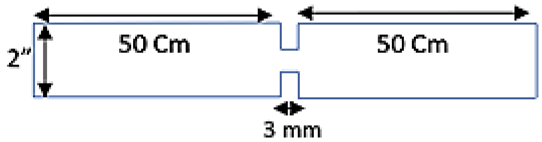

Fig. 1. Pipeline and Orifice dimensions.

Fig. 2 outlines the boundary conditions of a pipe; the left boundary is the flow inlet while the right boundary is the flow outlet. Inlet is a velocity inlet. Outlet is a pressure outlet. All other boundaries are walls with non-slip conditions. The velocity is varied based on flow rate.

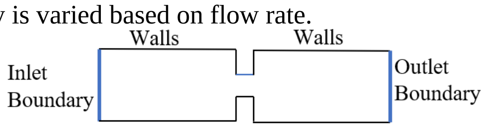

Fig. 2. Boundary Conditions.

Mesh independency was conducted to determine the optimal mesh size. 50 l/min flow rate was applied to a pipe of 2” diameter with orifice of 1”in the pipe, as shown in Fig. 2, So mesh of 285,508 cells, 574 faces, and 288,963 nodes is most suitable, Figs. 3 and 4.

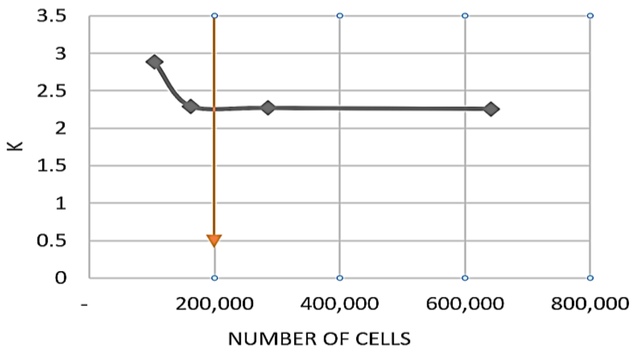

Fig. 3. Mesh Independency.

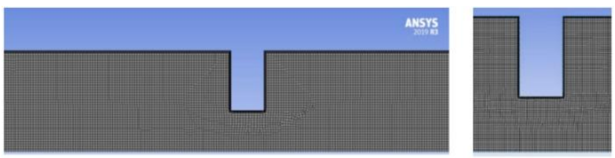

(a) (b)

Fig. 4. Mesh sizing of 0.25mm (a) Full Domain (b) zoomed in at Orifice.

Two-dimensional forced convection flow was modeled using ANSYS FLUENT 19 R3, discretization of second-order upwind interpolation, and the SIMPLE algorithm, k-ε turbulence model is used. Residual less than 8e-5 is obtained. Numerical results are validated using Tukiman et al. [14]'s. They focused on obtaining discharge coefficients and pressure drops for a specific diameter ratio of 2.4, obtaining results through different flow rates, and comparing the numerical data with published papers. Fig. 5 shows a comparison between the pressure drop of Turkish et al. [14] experimental results and current research. Fig. 6 shows comparison between the velocity contour and velocity vectors of Turkish et al. [14] experimental results and current research.

(a)

(b)

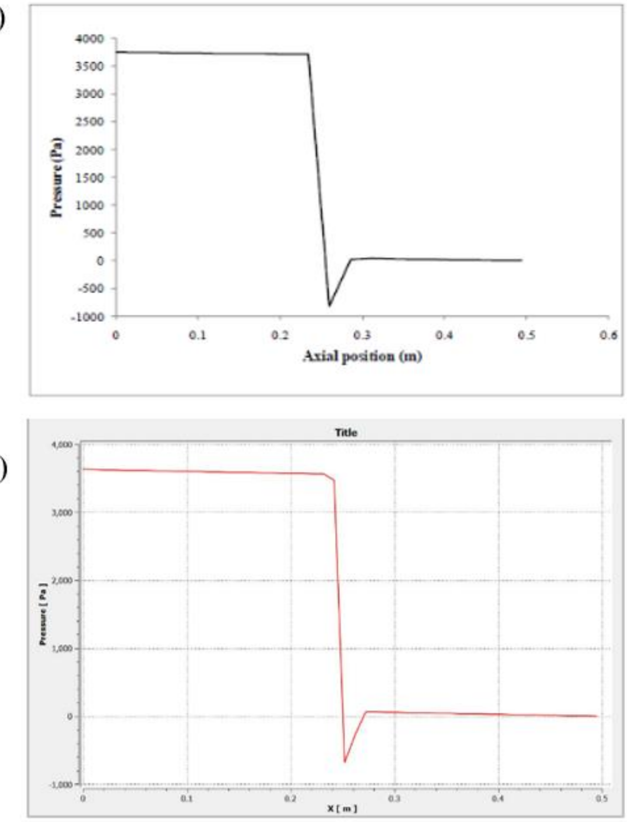

Fig. 5. Comparison between pressure drop of (a) Turkish et al. [14] Exp. (b) current research.

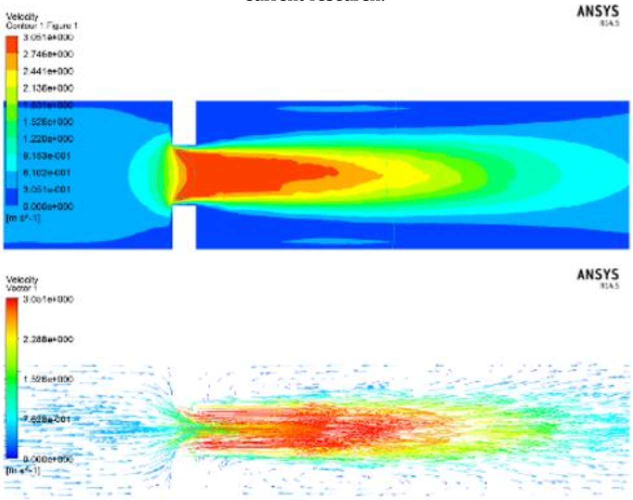

(a)

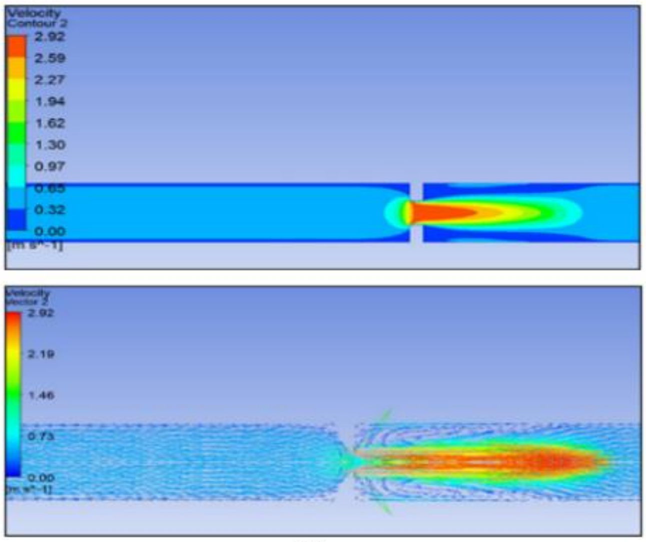

(b)

Fig. 6. Velocity contour and velocity vectors comparison between (a) Turkish et al. [14] Exp. (b) current research.

CFD simulations are made to predict the flow pattern through an orifice plate. Water cases use a flow rate of 50 lit/min. Pressure drops according to different diameter ratios. The main pipe is 2" diameter while the orifice diameters are 1", ¾", ½". Four orifices are started with but the 1/4" orifice encountered many problems. However, its results were canceled. Simulations results are obtained in terms of velocity profile, Figs. 7 to 9, K factor, Fig. 10, and pressure drop, Fig. 11.

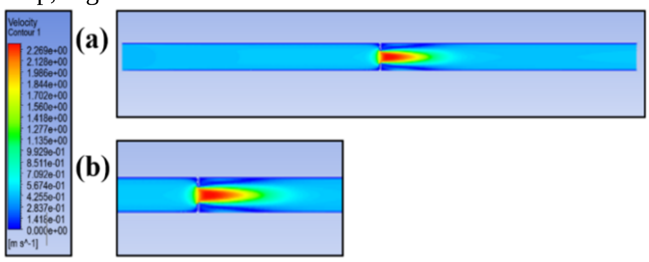

Fig. 7. Velocity distribution of Water flow passing through 1" orifice. (a) Full Domain (b) Domain (zoomed in).

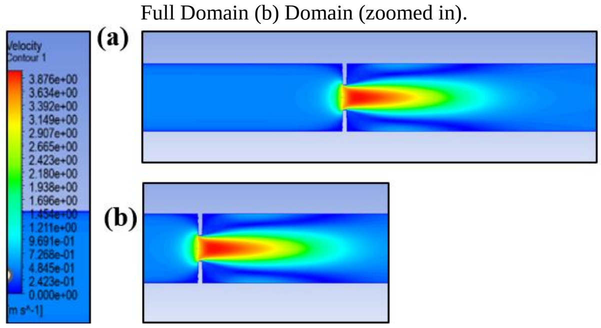

Fig. 8. Velocity distribution of the Water flow passing through 3/4" orifice (a) Full Domain (b) Domain (zoomed in).

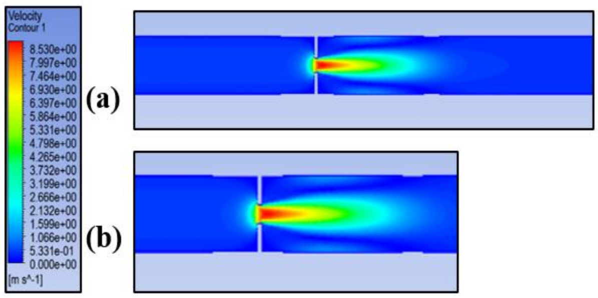

Fig. 9. Velocity distribution of the Water flow passing through 1/2" orifice (a) Full Domain (b) Domain (zoomed in).

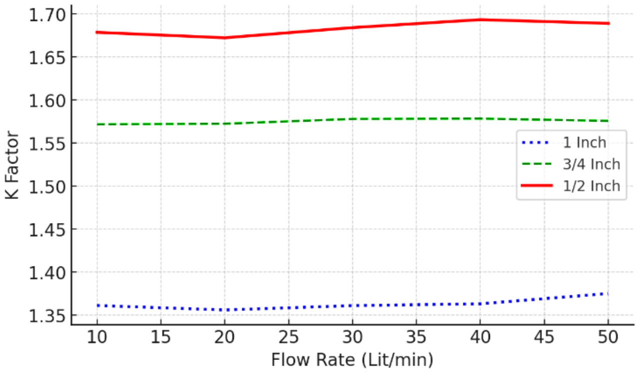

Fig. 10. Comparison between the water flow rate and K Factor for (1", ¾", and ½") orifices.

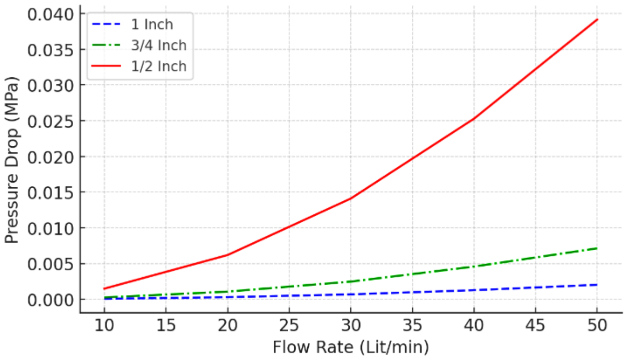

Fig. 11. Comparison between the water flow rate and Pressure drop for (1", ¾", and ½") orifices.

After applying pure water, the nanofluid mixture with a volume concentration (φ) of 4%, table 1, was simulated. Nanofluid simulations results are presented in terms of velocity profile, Figs. 12 to 14, K factor, Fig. 15, and pressure drop, Fig. 16.

TABLE 1: PHYSICAL PROPERTIES OF AL2O3 NANOPARTICLES:

Density **ρ** (kg/m^3)	Specific Heat **Cp** (J/Kg K)	Thermal Conductivity **K** (W/m K)	Viscosity **μ** (kg/m s)
3600	103,657	209,388	105,732

Equations (1) and (2) are used to determine nanofluid density and viscosity, respectively.

Density: $\rho_{nf} = \varphi\, \rho_p + (1\text{-}\varphi)\, \rho_{bf}$ (1)

Viscosity: $\mu_{nf} = \mu_{bf}\,(123\varphi^2 + 7.3\varphi + 1)$ (2)

Where ρ_{nf} and μ_{nf} are density and viscosity, respectively, of nanofluid; φ is the volume concentration, ρ_{bf} and μ_{bf} are density and viscosity, respectively, of base fluid, ρ_p is the density of nanoparticles.

From the equations (1) and (2) physical properties of Al_2O_3-H_2O nanofluid, table 2, has been calculated for a volumetric concentration of 4%.

TABLE 2: NANOPARTICLES AL2O3-H2O PROPERTIES (INPUT DATA TO ANSYS):

Materials	Density **ρ** (kg/m^3)	Viscosity **μ** (kg/m s)
Water H_2O	998.2	0.001003
Nanofluid Al_2O_3-H_2O	1086	0.000657

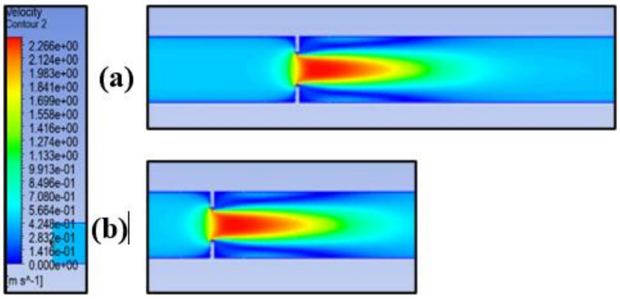

Fig. 12. Velocity distribution of Al_2O_3-H_2O flows passing through 1" orifice (a) Full Domain (b) Domain (zoomed in).

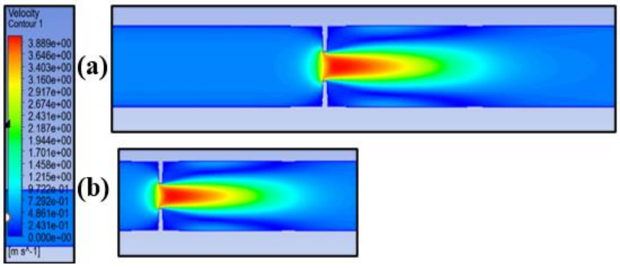

Fig. 13. Velocity distribution of Al_2O_3-H_2O flows passing through ¾" orifice (a) Full Domain (b) Domain (zoomed in).

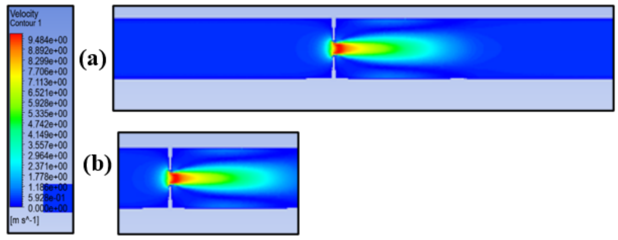

Fig. 14. Velocity distribution of Al_2O_3-H_2O flows passing ½" orifice (a) Full Domain (b) Domain (zoomed in).

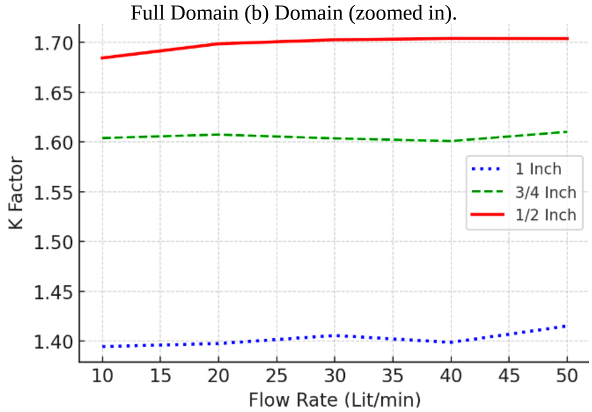

Fig. 15. Nanofluid Results Comparison between the flow rate and K Factor for (1", ¾", ½") orifices.

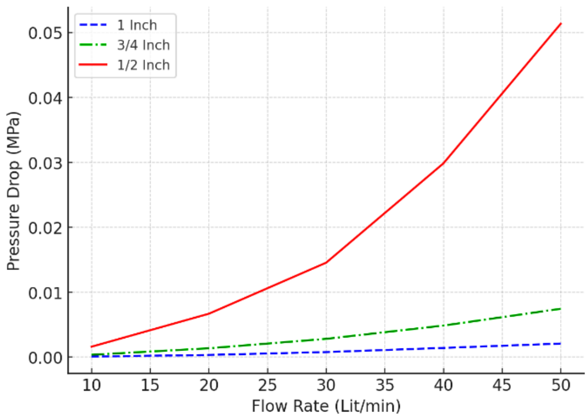

Fig. 16. Nanofluid Results Comparison between the flow rate and Pressure drop for (1", ¾", and ½") orifices.

Lots of cases had been conducted in order to compare the results while varying the flow rate. In this experiment, flow rate will be varied from 10 l/min to 50 l/min to evaluate orifice K loss factor in each case. Water of different flow rates had been applied. The same was done also for the Al_2O_3-H_2O. Nanofluid numerical results, Figs. 17 and 18, show higher values of pressure drop and k factor values, respectively.

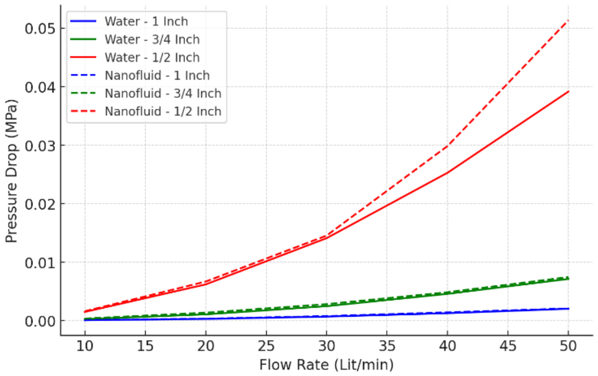

Fig. 17. Comparison between the flow rate and Pressure drop for (1”, ¾”, ½”) orifices.

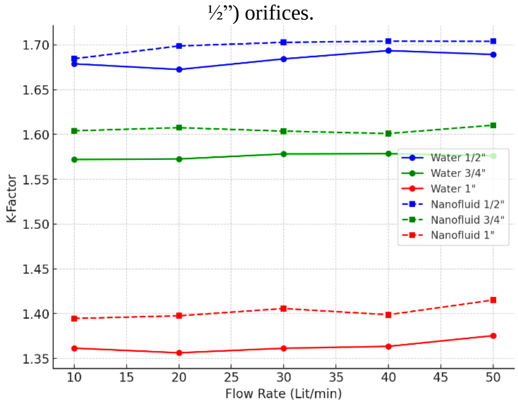

Fig. 18. Water vs Al_2O_3-H_2O Comparison between the flow rate and Pressure drop for (1”, ¾”, ½”) orifices.

To compensate for the pressure loss, the system needs additional pumping power. The pumping power is expressed in Equation (3).

$$Power = \eta\, P\, Q = \eta\, \rho\, g\, h\, Q \qquad (1)$$

Where, η : efficiency, P : pressure, Q : flowrate, ρ : density of fluid, g : gravity, and h : pressure head.

Fig.19 presents the effect of using Al_2O_3-H_2O nanofluids in comparison to water on the pumping power as a function of flow rate. It is observed that water exhibits lower pumping power compared to the nanofluid mixture. Al_2O_3-H_2O nanofluids has a higher density than pure water, which affected the pressure drop. The utilization of Al_2O_3-H_2O nanofluid instead of water leads to an increase in pumping power ranging from approximately 9% to 11%, respectively.

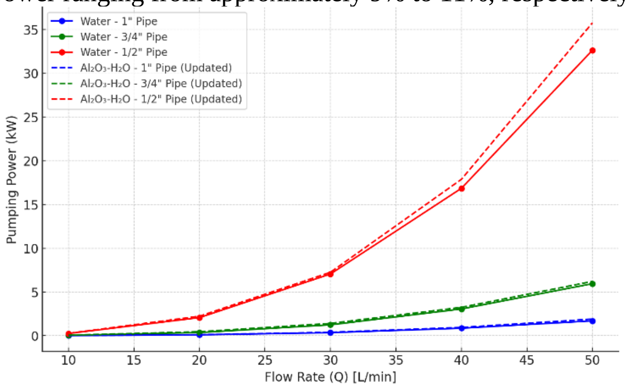

Fig. 19. Variation of Pressure drops with Flow rate for water and Al_2O_3-H_20 Mixture.

III. Experimental Analysis

Nanofluid properties can be tailored by adjusting two parameters; nanoparticle size and concentration. In this paper, Al_2O_3-H_2O nanofluid with particles of size 25 nm and a concentration of 0.04% will be used so that for 12 liters of base fluid 28.9 grams of nanofluid will be mixed together as shown in Fig. 20 (a). In this research, direct mixing and a magnetic stirrer will be utilized to ensure the best dispersion. The magnetic stirrer has a rotating magnet that mixes components, Fig. 20 (b). The base fluid is formed by mixing distilled water with ethylene glycol, acting as an antifoam and antifreeze material to prevent the mixture from failure.

(a) 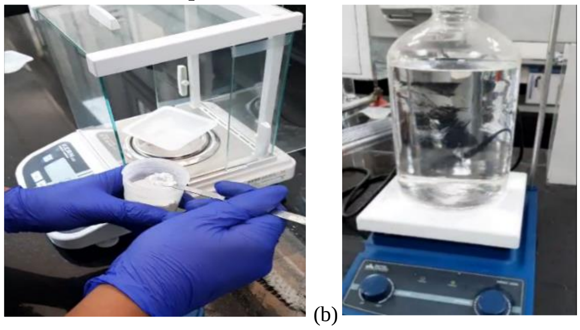 (b)

Fig. 20. Nanofluid Preparation (a) weigh a certain amount of nanofluid powder (b) mixing distilled water with ethylene glycol.

The stability of the nanofluid mixture is an important factor that affects the nanofluid’s properties. Nanoparticles always tend to aggregate, so the surfactant (Sodium Dodecyl Sulphate) was added to prevent aggregation and complete dispersion of the nanofluid mixture with ratio of 1:2 (1 gram of surfactant to 2 gm of nanoparticles), Fig. 21. Nanofluid does not last very long and the experiment was done immediately after preparation.

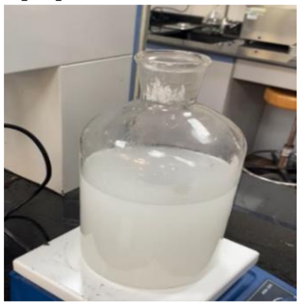

Fig. 21. Surfactant magnetic mixing with ratio 1:2.

The sonication process, which involves mixing ethylene glycol, water, sodium dodecyl sulphate, and nanoparticles, ensures complete homogenization and dispersion of the mixture after 30 minutes of sound energy agitation, Fig. 22.

Fig. 22. Sonication process for the nanofluid mixture

A real practical model is designed that will give an actual physical simulation of the CFD model, which facilitates the comparing process between water and nanofluid properties when passing through a piping network of the four orifices, Fig. 23.

Fig. 23. Piping Network.

The experiment used a pressure gauge to measure the pressure drop of a fluid through a series of polyvinyl chloride (PVC) pipes. The flow rate is calculated by filling a fixed volume of water in a specific time. The fluid is pumped by a 1 HP centrifugal pump through a closed loop cycle, connected to a plastic tank and piping system. The fluid flow and velocity are controlled by a 1 hp variable speed controller (dimmer controller) switch. Ball valves are used to control the flow direction and block it in specific situations, Fig. 24.

Fig. 24. Apparatus Setup

Orifices are used as fixed throttles. They generate head loss. In this apparatus, four orifice plates with different diameters are used 1”, ¾” and ½”, Fig. 25. Piping and orifices are joined together using steel flanges.

(a) (b) (c)

Fig. 25. Utilized Orifice Plates (a) 1” Orifice. (b) ¾” Orifice (c) ½” Orifice.

To determine pressure drop across the orifice, pressure gauges positioned at specific locations before and after the orifice were used. Pressure gauges are being positioned at a distance equal to twice the pipe diameter to ensure an accurate measurement. At this distance, the flow is stable and not affected by turbulence and to allow the pressure to stabilize after the disturbance caused by the orifice.

Many readings are taken and a series of valve openings (30%, 45%, 60%, 70%, and fully opened) to analyze the value of the loss coefficient factor K (dimensionless). It is required to specify the diameter in order to get the throat area as the used orifices diameters in the piping system (1”, ¾”, ½”, and ¼”).

Knowing the orifice throat area for each orifice, velocity can be calculated. Head loss is measured, and finally loss factor coefficient K can be calculated for water, Fig. 26, and nanofluid, Fig. 27.

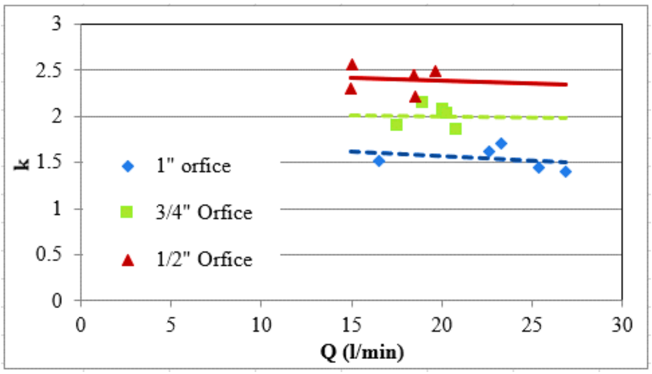

Fig. 26. Loss coefficient factor K values for water experimental results.

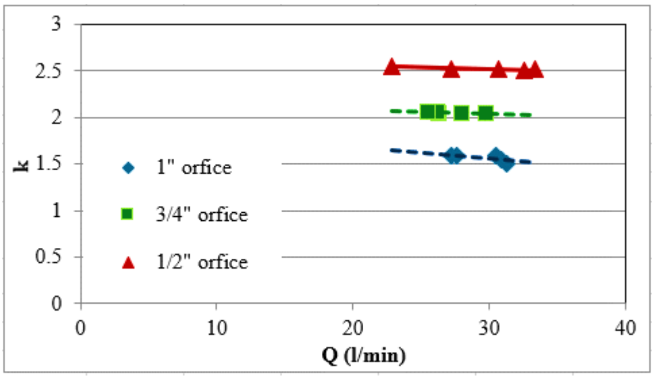

Fig. 27. Loss coefficient factor K for Nanofluid experimental results.

Figs. 28 to 30 show comparisons between experimental water and nanofluid mixture loss coefficient factor K for 1”, ¾” and ½”, respectively. It can be noticed that loss coefficient factor K values for nanofluid are always higher than those of water.

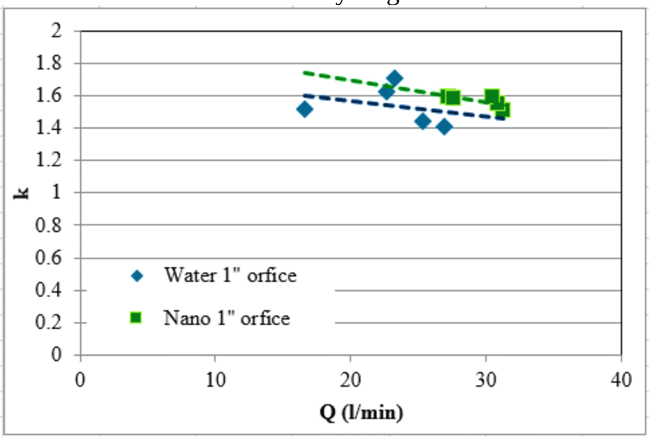

Fig. 28. Comparison between experimental Nanofluids and water K factors for 1” diameter orifice.

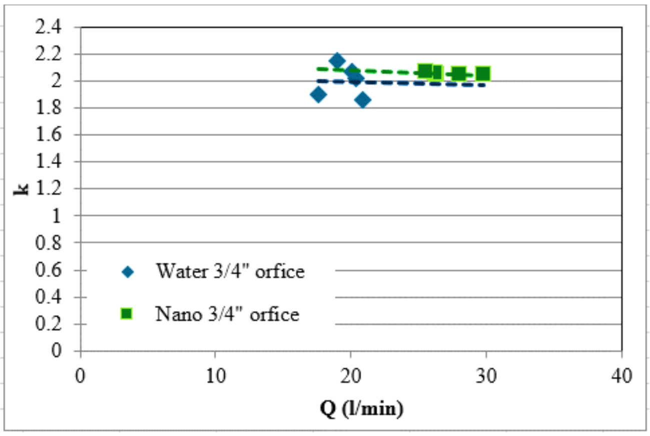

Fig. 2. Comparison between experimental Nanofluids and water K factors for 3/4" diameter orifice.

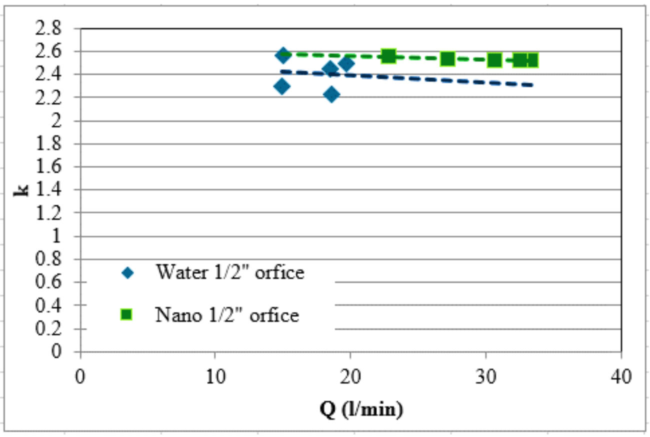

Fig. 30. Comparison between experimental Nanofluids and water K factors for 1/2" diameter orifice.

IV. CONCLUSION

In the current study, the pressure drop through orifices is numerically and experimentally analyzed for water and nanofluid Al_2O_3-H_2O. Loss coefficient factor K and pressure drop of nanofluids show slightly higher values than water results. Although nanofluids significantly enhance heat transfer rate and fluid properties, they also have a higher viscosity and density, which certainly affect the pressure drop and pumping power. A balance between heat transfer benefits and consumed power ensures a practical solution in industrial applications.

REFERENCES

1. Omar, A.K., Khaldi, A., and Ladouani, A., "Prediction of centrifugal pump performance using energy loss analysis", Australian Journal of Mechanical Engineering, vol. 15, issue 3, pp. 210-221, 2017.
2. Perissinotto, Rodolfo & Lazaro de Cerqueira, Rafael & Verde, William & Biazussi, Jorge & Bannwart, A.C. & Castro, Marcelo. (2022). Visualization of oil-water emulsion formation in a centrifugal pump stage.
3. Zhao, Lin & Chang, Zhuang & Zhang, Zhenduo & Huang, Rui & Denghui, He. (2021). Visualization of gas-liquid flow pattern in a centrifugal pump impeller and its influence on the pump performance. Measurement: Sensors. 13. https://doi.org/10.1016/j.measen.2020.100033
4. Perissinotto, R. M., Verde, W. M., Castro, M. S., Biazussi, J. L., Estevam, V., Bannwart, A. C., "Experimental investigation of oil drops behavior in dispersed oil-water two-phase flow within a centrifugal pump impeller", Experimental Thermal and Fluid Science, vol. 105, pp. 11–26, 2019. https://doi.org/10.1016/j.expthermflusci.2019.03.009
5. Perissinottoa, R. M., Verde, W. M., Perlesb, C. E., Biazussib, J. L., Castroa, M. S., Bannwarta, A. C., "Experimental analysis on the behavior of water drops dispersed in oil within a centrifugal pump impeller", Experimental Thermal and Fluid Science, vol. 112, 109969, 2020. https://doi.org/10.1016/j.expthermflusci.2019.109969
6. N. K. Chavda, J. P. Jani, A. K. Patel, K. P. Zala and N. G. Nimbark, "Effect of nano fluid on friction factor of pipe and pipe fittings: part I - effect of aluminum oxide nanofluid," International Journal of current Engineering and Technology, pp. 4039-4074, 2014.
7. S. U. Khalid, H. Babar, H. M. Ali, M. M. Janjua and M. A. Ali, "Heat pipes: progress in thermal performance enhancement for microelectronics," Journal of Thermal Analysis and Calorimetry, 143(3), pp. 2227-2243, 2021.
8. K. H. Do, H. J. Ha and S. P. Jang, "Thermal resistance of screen mesh wick heat pipes using the water-based Al2O3-H2O nanofluids," International Journal of Heat and Mass Transfer, p. 5888–5894, 2010.
9. H. M. Ali, H. Babar, T. R. Shah, M. U. Sajid, M. A. Qasim and S. Javed, "Preparation Techniques of TiO2 Nanofluids and Challenges: A Review," Applied Sciences, p. 587, 2018.
10. M. Ghanbarpour, E. B. Haghigi and R. Khodabandeh, "Thermal properties and rheological behavior of water based Al2O3-H2O ," Experimental Thermal and Fluid Science, pp. 227-235, 2014.
11. M. Shahrul, I. M. Mahbubul, R. Saidur, S. S. Khaleduzzaman, M. F. M. Sabri and M. . M. Rahman, "Effectiveness Study of a Shell and Tube Heat Exchanger Operated with Nanofluids at Different Mass Flow Rates," Numerical Heat Transfer, pp. 699-713, 2014.
12. J. L. Routbort, D. Singh, E. V. Timofeeva, W. Yu and D. M. France, "Pumping power of nanofluids in a flowing system," Journal of Nanoparticle Research, 13(3), pp. 931-937, 2011.
13. H. Babar and H. M. Ali, "Towards hybrid nanofluids: Preparation, thermophysical properties, applications, and challenges," Journal of Molecular Liquids, p. 598–633, 2019.
14. Tukiman, M. M., Ghazali, M. N. M., Sadikin, A., Nasir, N. F., Nordin, N., Sapit, A., & Razali, M. A. (2017, September). CFD simulation of flow through an orifice plate. In IOP Conference Series: Materials Science and Engineering (Vol. 243, No. 1, p. 012036). IOP Publishing.